AD________________

Award Number:
W81XWH-09-1-0322

TITLE:
Targeted Virus Nanoparticles for Localized Chemotherapy of Breast Cancer

PRINCIPAL INVESTIGATOR:
Junghae Suh, PhD

CONTRACTING ORGANIZATION:
Willliam Marsh Rice University

Houston, TX 77005

REPORT DATE:
October 2010

TYPE OF REPORT:
Annual

PREPARED FOR: **U.S. Army Medical Research and Materiel Command**
Fort Detrick, Maryland 21702-5012

DISTRIBUTION STATEMENT:

X Approved for public release; distribution unlimited

REPORT DOCUMENTATION PAGE

Form Approved
OMB No. 0704-0188

1. REPORT DATE *(DD-MM-YYYY)* 01-10-2010	**2. REPORT TYPE** ANNUAL	**3. DATES COVERED** *(From - To)* 15 SEP 2009 - 14 SEP 2010

4. TITLE AND SUBTITLE

Targeted Virus Nanoparticles for Localized Chemotherapy of Breast Cancer

5a. CONTRACT NUMBER

5b. GRANT NUMBER
W81XWH-09-1-0322

5c. PROGRAM ELEMENT NUMBER

6. AUTHOR(S)

Junghae Suh

5d. PROJECT NUMBER

5e. TASK NUMBER

5f. WORK UNIT NUMBER

7. PERFORMING ORGANIZATION NAME(S) AND ADDRESS(ES)

Willliam Marsh Rice University

Houston, TX 77005

8. PERFORMING ORGANIZATION REPORT NUMBER

9. SPONSORING / MONITORING AGENCY NAME(S) AND ADDRESS(ES)

U.S. Army Medical Research and Materiel Command

Fort Detrick, Maryland 21702-5012

10. SPONSOR/MONITOR'S ACRONYM(S)

11. SPONSOR/MONITOR'S REPORT NUMBER(S)

12. DISTRIBUTION / AVAILABILITY STATEMENT

Approved for public release; distribution unlimited

13. SUPPLEMENTARY NOTES

14. ABSTRACT

We aim to develop a new approach to treat breast cancer by targeting the commonalities that exist in all breast tissue (normal and malignant) to enhance delivery of chemotherapy to breast cancer and minimize delivery to non-breast tissue. We propose to create novel chemotherapeutic-carrying virus nanoparticles (VNPs) for localized drug delivery to breast tissue. We have successfully completed tasks 1-3 of our SOW. Specifically, we have attached paclitaxel on the AAV capsid at various ratios to create AAV-taxol conjugates, characterized the properties of the conjugates using a variety of assays to verify attachment, and created large diverse AAV capsid gene and particle libraries that are now ready to be used to select for virus variants with improved selectivity for breast cells. Highly targeted, multivalent drug delivery systems that can deliver chemotherapeutic drugs selectively to breast tissue cells have the potential to substantially improve the efficacy of chemotherapy while considerably reducing the magnitude of debilitating side effects.

15. SUBJECT TERMS

Drug delivery, chemotherapy, virus

16. SECURITY CLASSIFICATION OF:			**17. LIMITATION OF ABSTRACT**	**18. NUMBER OF PAGES**	**19a. NAME OF RESPONSIBLE PERSON** USAMRMC
a. REPORT U	**b. ABSTRACT** U	**c. THIS PAGE** U	UU	8	**19b. TELEPHONE NUMBER** *(include area code)*

Table of Contents

INTRODUCTION

Chemotherapy-related toxicities limit its maximal use. A main limitation is their non-discriminatory action towards normal organs in patients. Delivering drugs to breast cancer cells specifically is a considerable challenge. Previous strategies to identify markers specific for breast cancer cells often faced difficulties due to heterogeneity of cancer cells and similarities between cancer and non-cancer breast cells. We aim to develop a new approach to treat breast cancer by targeting the commonalities that exist in all breast tissue (normal and malignant) to enhance delivery of chemotherapy to breast cancer and minimize delivery to non-breast tissue. Our drug delivery platform is based on the adeno-associated virus (AAV), a 25 nm virus that is currently in clinical trials for a variety of gene therapy applications. We propose to create novel chemotherapeutic-carrying virus nanoparticles (VNPs) for localized drug delivery to breast tissue.

BODY

<u>Task #1</u>: Chemical conjugation of paclitaxel to virus scaffold

Paclitaxel was reacted with succinic anhydride to obtain taxol-2'-succinate. We attempted to use other one-step methods to synthesize taxol-NHS ester, but had difficulty getting rid of the DMSO from the product. So we used a two-step synthesis, and intermediate SDPP (N-hydroxy-succinimido diphenyl phosphate) was synthesized to increase the yield in step 3. Taxol-2'-succinate was reacted with SDPP to form taxol-NHS ester (Fig. 1).

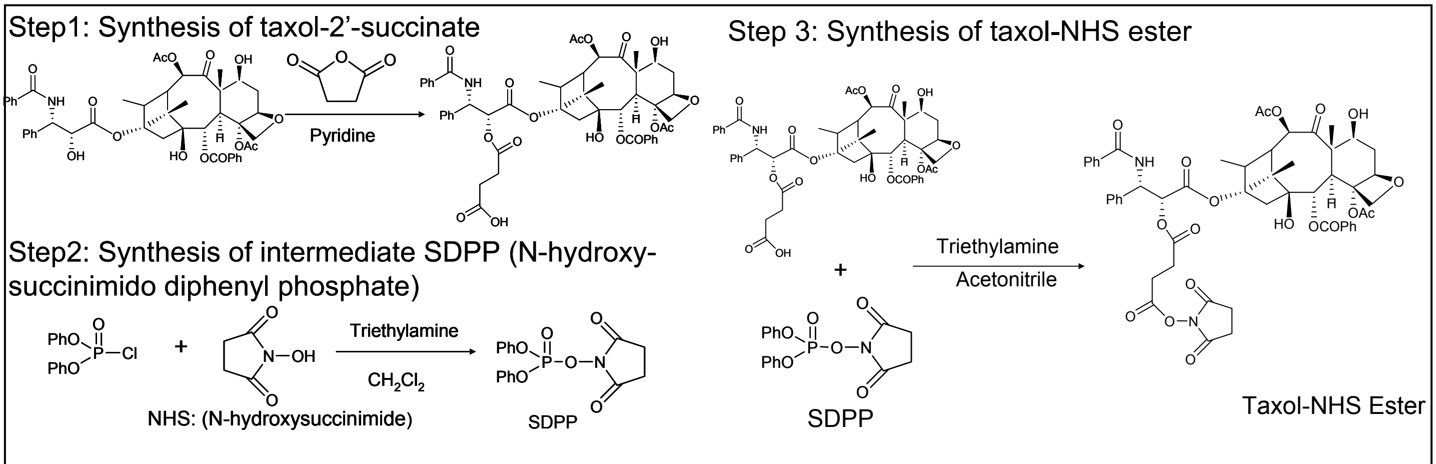

Figure 1. Steps to chemically synthesize taxol-NHS ester.

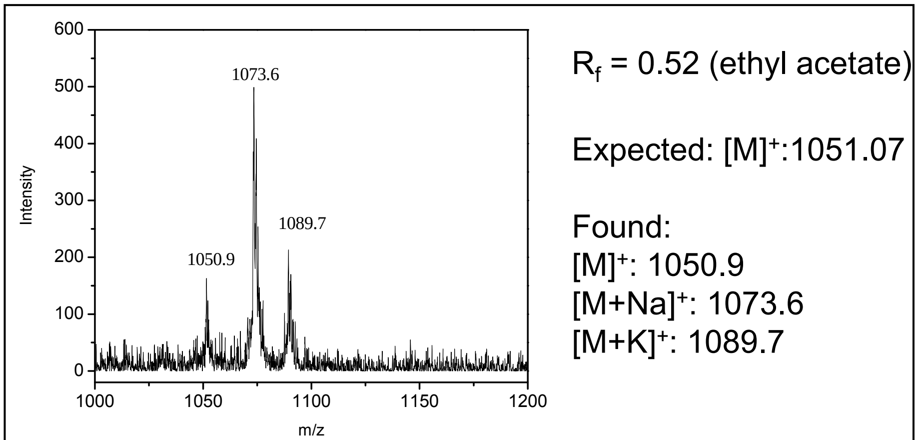

Figure 2. MALDI-MS analysis of taxol-NHS ester.

The taxol-NHS ester was purified by column chromatography using hexane and ethyl acetate as solvents. The purity of the product was confirmed by thin layer chromatography. The Rf value is 0.52 in ethyl acetate. The mass was confirmed with MALDI-MS (Fig. 2).

The taxol-NHS ester was reacted with AAV capsids at various molar ratios of taxol-NHS ester to lysine residues. There exist 1,080 lysine residues on the virus capsid. The reaction was done overnight at 4°C, with less than 10% DMSO in the final solution (Fig. 3). The reaction mixture was dialyzed against DPBS buffer to get rid of un-reacted taxol-NHS ester. Control experiments indicated that the AAV capsid is stable in 10% DMSO overnight. The TEM image in Figure 3 shows a virus capsid that was incubated in 10% DMSO overnight. No visible alterations to the virus capsid can be observed. Reaction was also tested with 4 hours reaction time instead of overnight, however no virus bands appeared in Western blots. Therefore, we decided to carry out the conjugation reactions overnight at 4°C.

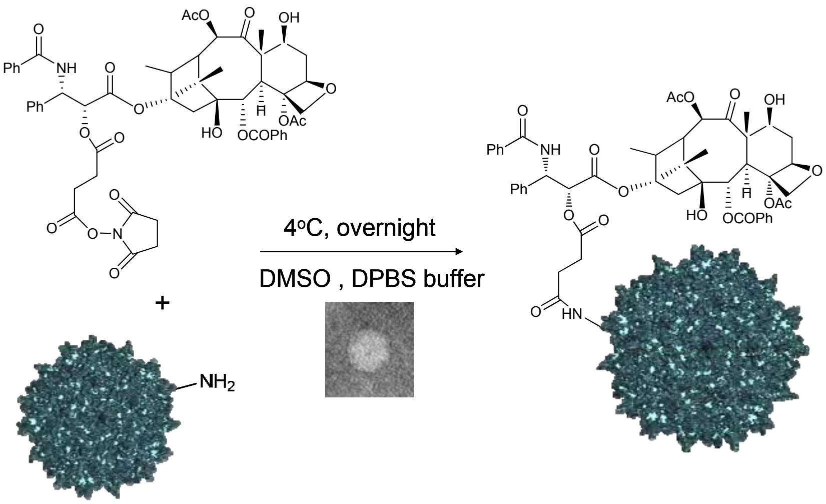

Figure 3. Conjugation of taxol-NHS ester to the AAV capsid.

TASK #2: Screen virus nanoparticles with conjugated paclitaxel

We attempted several times to use MALDI-TOF MS to analyze the AAV capsid with no success. Communication with other investigators in the field has revealed that AAV is an extremely challenging virus to analyze via MALDI-TOF. Thus, we pursued other methods to verify the conjugation of taxol onto the virus capsid.

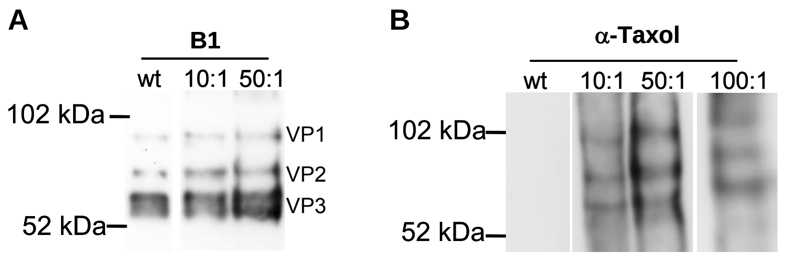

Figure 4. Western blots of denatured virus capsids conjugated with taxol at various ratios of taxol:lysine. (**A**) B1 antibody against the virus capsid subunits. Increased conjugation ratios result in increased protein molecular weight. (**B**) Anti-taxol antibody. Wild-type virus, as expected, yields no anti-taxol signal. Taxol staining for 10:1, 50:1, and 100:1 conjugation ratios indicates the presence of taxol molecules on VP subunits. Shifts in molecular weight again correspond to increasing conjugation ratios.

10:1

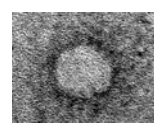

Figure 5. TEM image of an AAV capsid conjugated with taxol at a taxol:lysine ratio of 10:1.

To determine if taxol was successfully conjugated onto the AAV capsid, we ran two Western blots – one against the virus capsid subunits and the other against taxol. In the anti-capsid subunit blot (Fig. 4A), a slight increase in the sizes of VP1, VP2, and VP3 can be observed. When the blot was probed with an anti-taxol antibody, dramatic shifts in the sizes of all 3 subunits can be seen (Fig. 4B). At this point, it is unclear why the shifts observed in the 2 blots are not equivalent. One potential hypothesis is that there exists a heterogeneous mixture of subunits conjugated to varying degrees and the ones conjugated with detectable levels of taxol cannot be detected with the B1 antibody, perhaps due to masking of the B1 epitope. For Western blotting, samples were denatured and run on 7% Tris-Acetate gels. Protein was transferred to a nitrocellulose membrane and blocked with 5% skim milk for 1 h. Membranes were probed with primary antibody (1:200 dilution for B1 antibody, 1:100 dilution for anti-taxol antibody) for 1 h, rinsed, and probed with a horseradish peroxidase conjugated secondary antibody for 1 h. Images were taken using a FlourChem FC2 imager. TEM imaging of virus capsids conjugated with taxol suggest that the capsids are intact (Fig. 5).

Conjugation of taxol onto the virus capsid appears to prevent detection by the A20 antibody that detects intact capsids. In Figure 6A, a high titer of viral genomes/ml can be detected with QPCR for various conjugation ratios. However, ELISA with the A20 antibody fails to detect capsids for the 50:1 and 100:1 ratios. A dot blot with the A20 antibody confirms the lack of capsid detection for the higher conjugation ratio (Fig. 6B).

Taxol conjugation does not alter the binding of AAV to heparin, as reflected in the similar elution profile off of a heparin column (Fig. 7). This property was leveraged to remove un-reacted taxol from the AAV-taxol conjugates (see below).

To remove un-reacted taxol from AAV-taxol conjugates, we proposed using extensive dialysis against multiple buffer exchanges. Surprisingly, dialysis was not effective at removing free taxol. Figure 8A shows the results of a control experiment where free taxol alone was dialyzed overnight. When assayed on a dot blot, we see that the anti-taxol antibody is able to detect the presence of taxol in the dialyzed solution. When added to cells, the unremoved free taxol killed cells (Fig. 8B.b). To more effectively remove un-reacted taxol, we used heparin affinity column to purify the AAV-taxol conjugates. When the column purified conjugates were added to cells, they exhibited less acute cytotoxicity compared to the conjugates that were only dialyzed (Fig. 8B.c). Live/dead assays are underway to determine the percentage of dead cells in each of these cases. A size exclusion column will also be tested to removed un-reacted taxol-NHS ester. Therefore, we have concluded that dialysis alone does not remove unreacted taxol and an alternative separation/purification strategy is required to isolate the AAV-taxol conjugates.

A

Sample	ELISA (particles/ml)	QPCR (genomes/ml)
wt	3.75E+12	2.14E+12
10:1	1.16E+11	2.99E+11
50:1	0	8.05E+11
100:1	0	2.61E+11

B

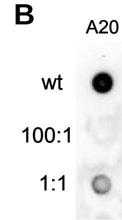

Figure 6. Detection of intact AAV capsids. (A) ELISA with the A20 antibody that detects intact capsids and QPCR with primers against the packaged virus genome. (B) Dot blot with the A20 antibody to detect intact capsids.

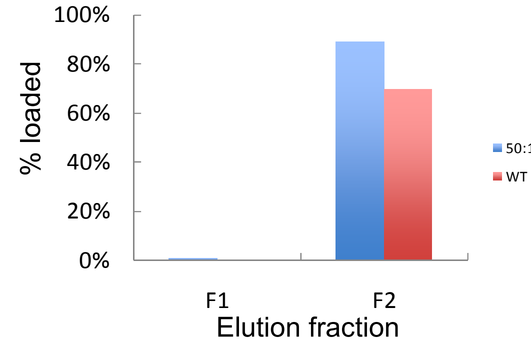

Figure 7. Heparin affinity assay. The AAV capsid conjugated with taxol at 50:1 ratio elutes from a heparin column similarly to wt capsid.

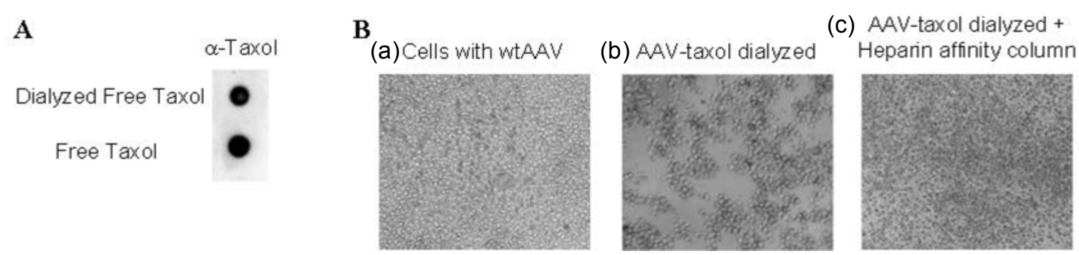

Figure 8. Problem with removing un-reacted taxol from the final product. (**A**) Dot blot of free taxol dialyzed overnight compared to un-dialyzed taxol. (**B**) HeLa cells with MOI of 40K, after four days infection. (a) Cells with wtAAV only. (b) Cells with dialyzed AAV-taxol. (c) Cells with heparin affinity column further purified AAV-taxol conjugation.

<u>TASK #3</u>: Generate diversity in virus nanoparticle library

<u>Error-prone PCR cap gene library</u>. We have optimized EP-PCR methods to generate a diverse gene library based on AAV2 *cap*. By altering the manganese chloride concentration in the PCR reaction, we are able to achieve different error rates (Table 1). Sequence analysis verifies that the mutations are unique to

Table 1. Error rates for different EP-PCR *cap* libraries. Transitions are changes from purines to purines (or pyrimidines to pyrimidines), transversions are changes from purines to pyrimidines (or vice versa), and insertions and deletions indicate addition or removal of nucleotides, respectively.

	50 μM $MnCl_2$	150 μM $MnCl_2$	250 μM $MnCl_2$	300 μM $MnCl_2$
Mutations per 1000 bp	3.1	5.8	16.8	20.4
Mutations per gene	6.82	12.76	36.96	44.88
% Transitions	56%	52%	39%	48%
% Transversions	44%	39%	39%	38%
% Insertion	0%	8%	10%	5%
% Deletion	0%	3%	12%	9%

each clone. With a 50 μM $MnCl_2$ concentration, we are able to achieve 3 mutations per 1000 bp with no insertions or deletions that may potentially alter the reading frame. The estimated diversity of our EP-PCR library is $9.7x10^5$, which is very close to our desired diversity of 10^6. This EP-PCR library can then be used with staggered extension process (StEP) as reported by Maheshri et al.(*1*) to further increase the genetic diversity in the library. Detailed properties of one of our EP-PCR AAV *cap* plasmid libraries is listed in Table 2.

Table 2. Properties of EP-PCR AAV *cap* library.

Basepairs Sequenced	**11,500**
Total Mutations	**41**
Total AA substituted	**31**
Mutation frequency, %	**0.36 +/- 0.24**
Mutations per gene	**8.2 +/- 5.5**
AA substitutions per gene	**6.2 +/- 4.7**
Mutation types, %	
A→T, T→A	**41.5**
A→C, T→G	**9.8**
A→G, T→C	**34.1**
G→A, C→T	**2.4**
G→C, C→G	**2.4**
G→T, C→A	**7.3**
Insertion	**2.4**
Deletion	**0**

Peptide display cap gene library. We have optimized peptide display methods to insert 7 random amino acids in to the tropism conferring domain of AAV2 *cap* as reported in Muller et al. (*2*) The sequences of 10 randomly selected clones are listed in Table 3 and verify that the virus gene library is diverse. There is no apparent pattern in the identities or types of amino acids that were inserted. An AAV peptide display library has been used previously by others to isolate virus variants that are able to transduce coronary artery cells which are normally resistant to AAV2 transduction.(*2*)

Table 3. Sequences of 10 randomly chosen peptide display virus gene clones.

Clone	Inserted nucleotides	Inserted Amino Acids
1	(Wild-type)	-
2	TTG GTT TCG TGT ACT GCT CTG	L-V-S-C-T-A-L
3	TGG ATT TTG AGA CTT GTA CTC	W-I-L-R-L-V-L
4	AAT AAT AAG ACG AAG AAT GCT	N-N-K-T-K-N-A
5	GCT ATT CTG CCG AAT ATT CTT	A-I-L-P-A-I-L
6	ACT GCT AGT TTT ATT AAG GTG	T-A-S-F-I-L-V
7	TGC CGA ATC ATT ATA CTT CTC	C-R-I-I-I-L-L
8	TTA TCG GCG GTT GCC TAA TCA	L-S-A-V-A-Stop-S
9	GGC AGA ATG GGG ATC CGA TGC	G-R-M-G-I-R-C
10	TAT CTT GAT TAT CTT TAT AAT	Y-L-D-Y-L-Y-N

Production of diverse AAV libraries. We have begun generating diverse AAV particle libraries based on the successful plasmid libraries. Table 4 lists the diversity and virus titers of several of our recently generated libraries. Plasmid Library EP 2 was generated with EP-PCR using 150 μM $MnCl_2$ and AAV2 *cap,* and has an error rate of around 6 mutations per 1000bp. Plasmid Library PD 1B was generated using peptide display and contains a random seven amino acid insert in the AAV2 heparin binding domain. As a first pass to create virus particle libraries with EP 2 and PD 1B plasmid libraries, 293T cells were transfected using a standard AAV transfection protocol using the library plasmid and pXX6 (encoding adenovirus helper functions). Due to virus capsid self-assembly, this protocol could allow for chimeric capsid formation if a single cell received more than one member of the library. Virus titers for these libraries, 1.99E12 and 3.37E11 genomes/mL, were above our minimum threshold of 1E11 genomes/mL. Next, we produced virus particle libraries EP 2 (S1) and EP 2 (S2) using a method to ensure that only one plasmid library member is delivered to each cell, greatly reducing the risk of chimeric capsids(*3*). In this method, a small amount of library plasmid is added and pBluescript is used as a 'stuffer' plasmid to facilitate the process. We are able to create very high titer virus libraries with this method (Table 4). In summary, we have successfully created high titer virus particle libraries using directed evolution. The libraries are ready to be used in positive selection procedures to isolate mutants able to transduce breast cells with higher efficiency. Future work will also include using virus libraries of lower error rates, in case of EP-PCR, to minimize the potential of protein structure destabilizing mutations.

Table 4. Diversity and titer of AAV libraries.

Library Designation	Plasmid Library Diversity	Viral Titer (genomes/mL)
EP 2	5.00E+05	1.99E+12
EP 2 (S1)	5.00E+05	3.12E+12
EP 2 (S2)	5.00E+05	2.55E+12
PD 1B	1.00E+03	3.37E+11

KEY RESEARCH ACCOMPLISHMENTS

- Synthesized taxol-2'-succinate, purified the product and confirmed the product by MALDI-MS.
- Synthesized taxol-NHS ester, purified the product with column chromatography and confirmed by MALDI-MS.
- Conjugated taxol to AAV capsid surface through ester bonds. Conjugation was confirmed by Western blots using B1 and taxol antibodies.

- Generated large diverse AAV capsid gene libraries using peptide display and error-prone PCR.
- Generated large AAV particle libraries ready to be used for selection on breast cells.

REPORTABLE OUTCOMES

Presentations	• "Targeted Adeno-Associated Virus (AAV) Nanoparticles for Localized Chemotherapy of Breast Cancer" oral presentation at Biomedical Engineering Society (BMES) annual meeting, Austin, Texas, 9 October, 2010. • "Targeted Adeno-Associated Virus (AAV) Nanoparticles for Localized Chemotherapy of Breast Cancer" oral presentation at American Institute of Chemical Engineers (AIChE) annual meeting, Salt Lake City, Utah, 11 November, 2010.

CONCLUSION

We have successfully completed tasks 1-3 of our Statement of Work. Specifically, we have attached paclitaxel on the AAV capsid at various ratios to create AAV-taxol conjugates, characterized the properties of the conjugates using a variety of assays to verify attachment, and created large diverse AAV capsid gene and particle libraries that are now ready to be used to select for virus variants with improved selectivity for breast cells. Highly targeted, multivalent drug delivery systems that can deliver chemotherapeutic drugs selectively to breast tissue cells have the potential to substantially improve the efficacy of chemotherapy while considerably reducing the magnitude of debilitating side effects.

REFERENCES

1. N. Maheshri, J. T. Koerber, B. K. Kaspar, D. V. Schaffer, *Nat Biotechnol* 24, 198 (Feb, 2006).
2. O. J. Muller *et al.*, *Nat Biotechnol* 21, 1040 (Sep, 2003).
3. J. T. Koerber, N. Maheshri, B. K. Kaspar, D. V. Schaffer, *Nat Protoc* 1, 701 (2006).